John von Neumann Institute for Computing

Ab Initio Study of Pr Oxides for CMOS Technology

Jarek Dąbrowski, Victor Zavodinsky

published in

NIC Symposium 2004, Proceedings,
Dietrich Wolf, Gernot Münster, Manfred Kremer (Editors),
John von Neumann Institute for Computing, Jülich,
NIC Series, Vol. **20**, ISBN 3-00-012372-5, pp. 171-180, 2003.

http://www.fz-juelich.de/nic-series/volume20

Ab Initio Study of Pr Oxides for CMOS Technology

Jarek Dąbrowski[1] **and Victor Zavodinsky**[1,2]

[1] IHP, Im Technologiepark 25, 15236 Frankfurt (Oder), Germany
E-mail: dabrowski@ihp-ffo.de, zavodins@iacp.vl.ru

[2] Institute of Materials Sciences, 153 Tikhookeanskaya
680042, Khabarovsk, Russia

We performed *ab initio* pseudopotential DFT calculations providing insight into the atomic structures and processes responsible for the quality of alternative gate dielectrics in deep sub-100 nm CMOS technologies. Here we summarize our results on point defects in Pr_2O_3, on the interface structure between Pr oxides and Si(001), and on the interface oxidation and formation mechanism of the interfacial layer.

1 Introduction

Scaling of Complementary Metal-Oxide-Semiconductor (CMOS) devices requires gate oxide-equivalent thickness $t_{\rm eq} < 1.5$ nm for the 70 nm technology node. Experts predict that integrated circuits containing such small devices will be on the market already by the year 2008. Since direct tunneling increases exponentially with decreasing oxide thickness, gate dielectrics with $t_{\rm eq}$ significantly below 2 nm can be of practical use only if an alternative insulator with dielectric constant K of 20-40 is introduced (the dielectric constant of SiO_2 is $\sim$4), so that the physical thickness of the insulator can be increased[1]. A key parameter for circuit designers is the current which can flow through the transistor; this current is proportional to the gate capacitance C, thus defining the required value of C. The latter can be realized by using a classical SiO_2 gate oxide with physical thickness $t_{\rm ox} = K_{\rm ox}/C$ or an alternative dielectric with the dielectric constant K and physical thickness $t = K/C$. This means that by increasing the dielectric constant n times one can increase n times the physical thickness of the insulator. Hf and Pr oxides are among the major candidates for high-K gate dielectrics. Here we focus on Pr_2O_3[2–6].

2 Motivation

The purpose of the calculations is to assist development of gate dielectrics for new generations of MOS transistors[1]. The primary practical issue is to achieve the Equivalent Oxide Thickness[a], EOT as low as 1 nm and less. EOT is associated with general features of the film morphology. In particular, the chemical composition of the film is a function of the distance from the substrate[8,7,9,10], which affects the effective dielectric constant of the film. In addition to EOT reduction, the density of charge traps (fixed and reloadable) in the film and at the interface must be brought down to a value comparable to that typical for industrial quality gate SiO_2. Charge trap densities are a derivative of film morphology,

[a] Thickness of SiO_2 with the capacity equal to the capacity of the alternative dielectric layer.

being associated with particular processing steps needed to produce a film with a given stoichiometry distribution, and with the structure and composition of the film.

Reduction of the EOT to the target value is a major technological and scientific problem. EOT is increased by oxidation of the substrate during the growth and by the presence of a silicate layer at the interface (Pr silicate has a noticeably lower dielectric constant than Pr_2O_3). To this end, we have addressed several issues. We have:

- established a low-energy model of chemically sharp Pr_2O_3(110)/Si(001) interface;
- analysed energetics of substrate oxidation in the pre-amorphous regime;
- examined structural models for quasi-crystalline interfacial silicates;
- approximated the range of O chemical potential where Pr_2O_3 and SiO_2 mix;
- proposed a conceptual model for the interfacial silicate formation.

The second group of problems has to do with the need to reduce the density of charge traps (reloadable and fixed) to the value comparable to that typical for industrial quality gate SiO_2/Si(001). The physical origin of these difficulties is less clear at the moment. We have made an attempt to estimate the viability of various types of defects (including Si dangling bonds[b]) as charge traps. So far, we have:

- computed electrical activity and formation energies of several point defects in Pr_2O_3,
- considered several interfacial defects involving Si dangling bonds,
- estimated the misfit defect density at the interface given total energy differences and force constants available from the calculations.

3 Approach

The calculations were done by the *ab initio* pseudopotential plane wave code fhi96md[11]. We applied the Local Density Approximation (LDA) for the exchange and correlation energy[12,13] and nonlocal pseudopotentials in the Troulller-Martins scheme[14,15] with 40 Ry cutoff for plane waves. The Brillouin zone was sampled at the special k-point set corresponding to the (1/4, 1/4, 0) point from the first Brillouin zone of Si(001) 3×3 surface cell (interface calculations) or at the Γ point of the cubic Pr_2O_3 80-atom cell (bulk calculations). Pr_2O_3/Si(001) films were modelled by periodically repeated slabs consisting of six Si layers and up to four layers of oxide. The Si substrate was terminated on one side by hydrogen and the slabs were separated by 10 Å of vacuum. We computed total energies and electronic structures for numerous interface and film structures and for various stoichiometries.

Because of the open f-shell of Pr atoms, a key problem in calculations involving Pr is in construction of a reliable Pr pseudopotential[3,16,17]. It turns out that two different Pr pseudopotentials are needed: a pseudopotential with two core f electrons for Pr_2O_3 (trivalent Pr(III), +3 ionic charge), and with only one f electron for PrO_2(tetravalent Pr(IV), +4 ionic charge). Thus, Pr^{+3} and Pr^{+4} are treated by us as distinct species. We calibrate the pseudopotential energy difference such that the experimental difference in formation enthalpies of Pr_2O_3 and PrO_2 is reproduced[18]. The fundamental bulk properties (lattice constant, bulk modulus) of Pr_2O_3 and PrO_2 obtained with these pseudopotentials are in agreement with experimental data; the discrepancies are well within the range typical for LDA calculations.

[b] It is known that Si dangling bonds are responsible for reloadable traps at SiO_2/Si interfaces

4 Bulk Pr Oxides

The simplest Pr oxide is PrO_2. It crystalizes in the CaF_2 structururе which can be viewed as the zinc blende structure with anion sites occupied by Ca (or praseodymium) atoms, and the cation and tetrahedral interstitial sites occuped by F (or oxygen) atoms. Thus, every Pr atom is eightfold-coordinated and every O atom is fourfold coordinated. All Pr atoms in PrO_2 are Pr(IV) and each has transferred four electrons to oxygen atoms. When a quater of the oxygen atoms is removed from the crystal, this charge transfer is reduced to three electrons per metal atom and Pr_2O_3 with Pr(III) is formed. The atomc structure of Pr_2O_3 remains closely related to that of PrO_2: the oxygen vacancies are ordered in a $2\times2\times2$ simple cubic array made of Pr fcc cubes, each fcc cube containing two O vacancies. In this way, every Pr atom has now six O neighbors and every O atom retains four Pr neighbors.

The typical composition of praseodymium oxide is Pr_6O_{11}, corresponding to an ordered $(Pr_2O_3)\cdot4(PrO_2)$ phase[20]. Cubic Pr_2O_3 is stable under high vacuum[21]. When deposited on Si(001) by electron beam evaporation, it grows with the (110) axis normal to the substrate. PrO_2 films on Si have not been reported. Therefore, our calculations are done nearly exclusively for Pr_2O_3; the dioxide is treated only as a reference to calibrate the pseudopotential for tetravalent Pr. This is necessary because one cannot apriori exclude that Pr(IV) atoms appear in certain structures of the interfacial region. However, up to now we have not identified any structures containing Pr(IV) which are stable under the conditions during growth and annealing of MBE Pr oxide layers.

The calculated lattice constant of Pr_2O_3 is 11.074 Å, less by 0.33% than the experimental 11.115 Å[19], and the bulk modulus is 280 GPa. LDA calculations yield 2.0 eV for the offset between bulk Si and bulk Pr_2O_3 valence band maxima.

5 Formation of the Interfacial Layer

A good matching between lattice spacings of the oxide and of the Si(001) substrate occurs when the (110) axis of the oxide is normal to the substrate, and the (100) axis of the film is parallel to the (110) axis of the substrate. In this configuration, each three Si atoms find a corresponding pair of Pr atoms. Two of these three Si atoms become now dimerized, which leaves the Si surface with four dangling bonds per each 3×1 unit, that is, two Si dangling bonds per each Pr atom on the oxide side. If the oxide had the composition of PrO_2, this would mean that there are four oxygen atoms per these two Pr atoms; the position of these O atoms would roughly match the position of the dangling bonds bonds and each of the interfacial Si atoms could be oxidized. However, in Pr_2O_3 stoichiometry there are only three O atoms available for this purpose, leaving in each 3×1 unit one Si dangling bond without an oxygen partner.

An additional important factor is a charge mismatch between these materials. Bulk Pr_2O_3 is strongly ionic: one can assume that each Pr atom gives three electrons away and each O atom captures two electrons. But since O atoms at the interface form bonds (predominantly covalent) with Si atoms, they are only partially involved in the charge transfer from metal atoms. As a consequence, each interfacial Pr_2O_3 moiety donates two electrons which cannot be localized on the existing anions if the oxide is stoichiometric.

We find that in the ideal case of pure Pr_2O_3/Si(001) film (no silicate) these electrons are trapped by additional O located in the second Pr layer. This basic model, constituting

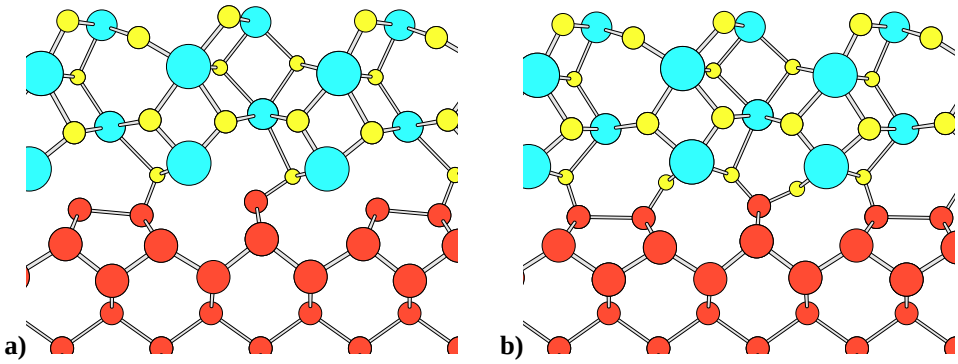

Figure 1. Fundamental interface structures of Pr_2O_3/Si(001). Si atoms are red, O atoms are yellow, Pr atoms are blue. Electron densities of state are semiconducting, with clean gap. **(a)** Stoichiometric interface. This system has one Si dangling bond (electrically inactive) per interfacial Pr atom, or two per 3×1 unit. The interfacial Pr layer has 1/3 deficiency in oxygen, the next Pr layer is enriched in oxygen by 1/3, and the remaining layers are stoichiometric. In Fig. 2, this structure is labelled 2(SiPr). **(b)** Interface enriched with oxygen. The dangling bonds are oxidized, and both the interfacial and the next-to-interfacial Pr layers are rich in ogygen; nevertheless, all Pr atoms are in Pr^{+3} charge state. In Fig. 2, this structure is labelled 0(SiPr).

the starting point of analysis of the system, is illustrated in Fig. 1a for stoichiometric oxide and in Fig. 1b for oxygen rich oxide. In stoichiometric Pr_2O_3/Si(001) one of the interface O atoms moves from Si–O–Pr site into the film, leaving behind a SiPr "bond", i.e., a Si^{-1} ion forming a mostly ionic bond to two Pr^{+3} neighbors (Fig. 1a). This dangling bond is not a source of trapped charge, because the electrostatic interaction with the positively charged neighbors moves the (0/-) transition state into the valence band of silicon.

5.1 Energetics of Substrate Oxidation

During MBE deposition by electron beam evaporation from a Pr oxide source, the growing film is in contact with vapor consisting of PrO molecules and O atoms. In practice, this means that the system is exposed to an oxidizing envoronnemt. Indeed, noticeable Si oxidation takes place unless the substrate temperature is so low that the Pr oxide film grows amorphous. When the tepmerature is high enough for epitaxial growth (e.g., 500°C), some oxygen atoms arrive at the substrate and react there.

In this Section we discuss oxygen incorporation energies at various interfacial sites. We also consider oxygen-poor stoichiometries.

Fig. 2 collects formation energies of many interfacial structures, shown as a function of oxygen chemical potential μ(O). Zero of the formation energy refers to the fully oxidized boundary (Fig. 1b), and zero of μ(O) is chosen at equilibrium with SiO_2. The number of Pr atoms is the same in all structures, but in general, thermal equilibrium requires that:

$$\mu(\mathrm{Pr}) + 1.5\mu(\mathrm{O}) = \Delta G_f(\mathrm{PrO}_{1.5}) - 0.5\Delta G_f(\mathrm{SiO}_2), \qquad (1)$$

where the ΔG_f stands for Gibbs formation energy of a compound and the term $0.5\Delta G_f(\mathrm{SiO}_2)$ is added because the standard formation energy of Pr_2O_3 is measured with

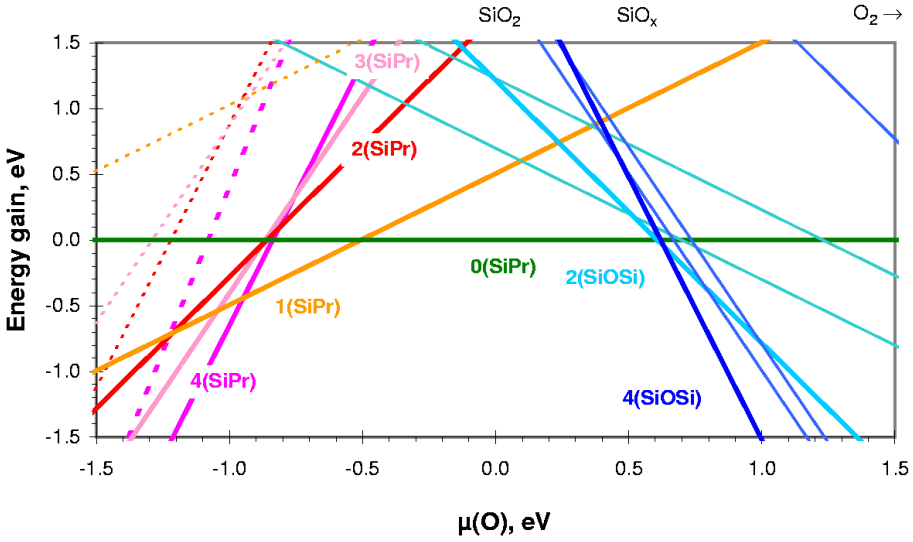

Figure 2. Stability of Pr_2O_3/Si(001) interface structures as a function of oxygen chemical potential μ(O). Note that zero of the chemical potential is chosen at the equilibrium with SiO_2; $0.5\mu(O_2)$ is thus far on the right-hand side, at μ=4.9 eV (LDA value). Bold lines correspond to the structures discussed in the text. The labels associate each structure with its characteristic feature: n(SiPr) means that there are n SiPr interfacial units per each 3×1 unit, and n(SiOSi) means that there are n units on the Si side.

respect to O_2, not SiO_2. The left-hand end of the diagram represents the oxygen-poor limit, roughly corresponding to μ(Pr)=0, that is, to the equilibrium with Pr metal.

Let us go through Fig. 2 from the oxygen poor to the oxygen rich limit, focusing on the structures with the lowest energies. The interface labelled 4(SiPr) has four SiPr units in each 3×1 cell, that is, there is no oxygen between interfacial Si and Pr atoms. These interfacial SiPr sites are the first to be oxidized. The energy of oxygen incorporated into such a site depends on the local geometry (dimerized or undimerized Si atom) and on the total number of incorporated oxygen atoms and varies between -1.2 and -0.5 eV. Si–Si bonds are oxidized next. Due to geometry constraints, O incorporated into a surface Si–Si bond has energy by $\sim$0.6 eV higher than in SiO_2. This can be viewed as the onset of SiO_x formation. Oxidation of subsurface Si–Si bonds leads to further stress accumulation, Si ejection, and eventually to formation of amorphized SiO_2 interfacial layer.

5.2 Silicide Formation

Although we did not calculate silicide structures explicitely, the left-hand side of the diagram in Fig. 2 strongly suggests the stability of the film with respect to silicide formation. This conclusion comes from a simple comparison of formation energies computed for interfacial structures containing SiPr bonds (silicide type) and PrOSi bonds (silicate type). A stoichiometric interface has 50% of the interfacial bonds of silicide and 50% of silicate type (Fig. 1a). O atoms are removed from the film in the oxide poor regime, when μ drops below μ_{PrOPr} = -2.3 eV. At more oxidizing conditions, when μ rises above μ_{PrOSi} = -1.0 eV, oxygen is inserted into interfacial PrSi bonds. Since the energy of O is lower between

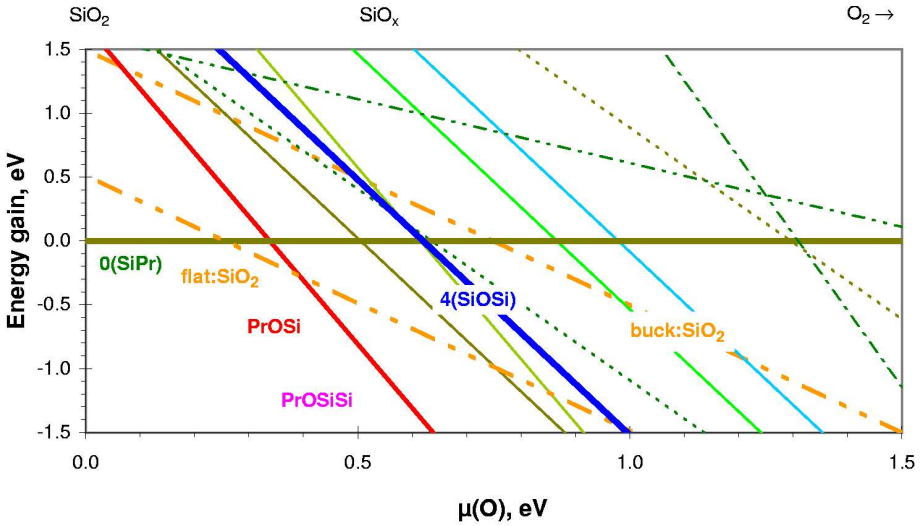

Figure 3. Stability of silicate structures at the Pr_2O_3/Si(001) interface as a function of oxygen chemical potential μ(O). Bold lines correspond to the structures discussed in the text. The labels associate each structure with its characteristic feature: buck:SiO_2 and flat:SiO_2 refer to SiO_2 molecules dissolved in an ultrathin film unrer a buckled and a flat surface (Fig. 4a-b), "PrOSi" indicates the presence of mostly PrOSi bonds in an intercalating SiO_2 layer (Fig. 4c) and "PrOSiSi" indicates that SiSi bonds occur in a thicker intercalating SiO_2 layer (Fig. 4d). The structures 0(SiPr) and 4(SiOSi) are the same as in Fig. 2.

Pr and Si atoms than between two Si atoms (by 1.0 eV), silicide can be formed only when not enough O is available. Otherwise, O is extracted from SiOSi bonds and inserted between Si and Pr, reducing the Si (sub)oxide and oxidizing the silicide.

5.3 Silicate Formation

We now consider the possibility of silicate formation at the interface. We computed total energies for numerous simplified models of interfacial silicates, differing in stoichiometry, atomic arrangement, and imposed lateral periodicity (from 3×1 to 3×3, measured in Si(001) surface lattice constant). Most of these structures are clearly unstable, that is, their energies fall well above the lowest energies of silicate-free film at any realistic value of oxygen chemical potential. However, some of the structures turned out to be stable for O chemical potential in the SiO_x range (Fig. 3). This is in spite of the fact that the small cell sizes used (for practical reasons) in the calculation have most certainly lead to accumulation of lateral stress in the silicate layer.

When a SiO_2 molecule dissolves in Pr_2O_3, two O^{-2} atoms are substituted by a $(SiO_2)^{-4}$ moiety. In other words, two O atoms are removed from the film to the reservoir of O with energy μ, a Si atom is added from Si bulk, and four O atoms are taken from the reservoir and placed between Pr and Si. If Si is in equilibrium with Si bulk and O is in equilibrium with the reservoir, we can thus estimate the silicate formation energy $E_{\rm f}$ from

$$E_{\rm f} = (2\mu_{\rm PrOPr} - 2\mu) + (4\mu - 4\mu_{\rm PrOSi}) \simeq 2\mu - 0.6{\rm eV}, \qquad (2)$$

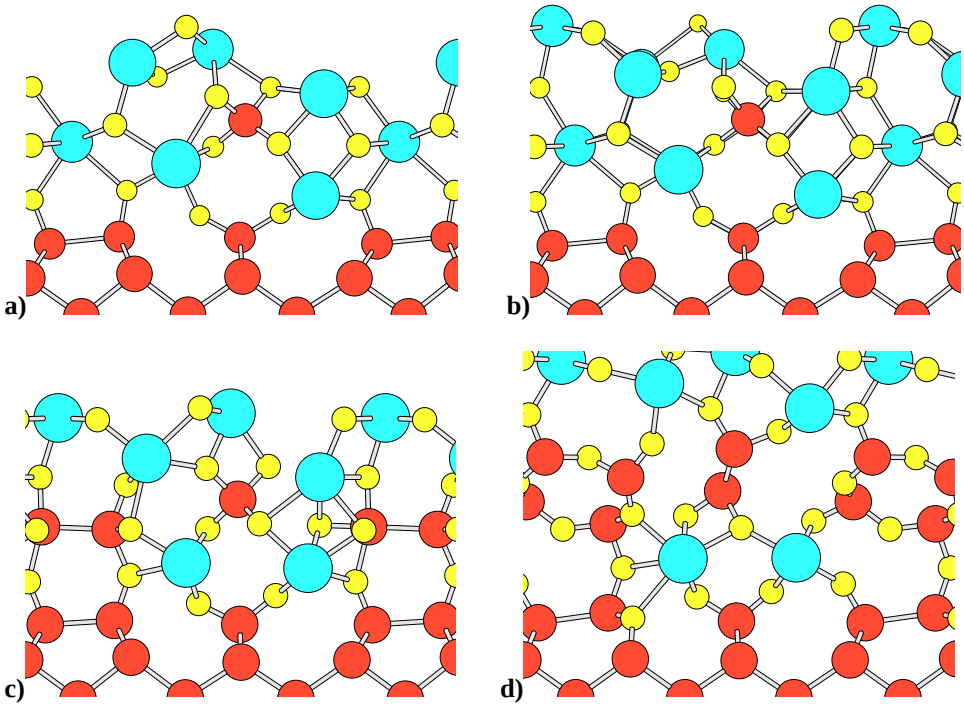

Figure 4. **(a)** A SiO_2 molecule buckles the surface of the ultrathin Pr_2O_3 film. This structure is labelled buck:SiO_2 in Fig. 3. **(b)** Filling the trenches with 0.5 monolayer Pr_2O_3 flattens the surface and reduces the energy. This structure is labelled flat:SiO_2 in Fig. 3. **(c)** A monolayer of Si oxide intercalated above the first Pr_2O_3 layer. Most of the bonds of the intercalate are of silicate character. This structure is labelled PrOSi in Fig. 3. **(d)** . Additional two monolayers of Si suboxide intercalated above the first Pr_2O_3 layer. There are SiSi bonds in the intercalate. This structure is labelled PrOSiSi in Fig. 3.

where the energy of O in the film is approximated by μ_{PrOPr}. Positive E_{f} means that the silicate is stable. It follows that already at $\mu \simeq 0.3\,\mathrm{eV}$ a process collecting two O atoms on a Si atom and dissolving the resulting SiO_2 moiety in the Pr_2O_3 film is expected to be energetically favorable, due to low energy of oxygen between Pr and Si atoms (μ_{PrOSi}).

The estimate of Eq. 2 is confirmed by a direct calculation for a SiO_2 molecule dissolved in a 3 monolayer thick Pr_2O_3/Si(001) film. Silicate formation begins at $\mu_1 = 0.8\,\mathrm{eV}$ when the film surface buckles due to the additional volume introduced by the SiO_2 molecule, and at $\mu_2 = 0.3\,\mathrm{eV}$ when the surface is made smoother by depositing half a monolayer of Pr_2O_3 (Fig. 4a-b). This formation energy difference turns out to be equal to $\Delta E_{0.5} = E_4 - E_{3.5} = E_{3.5} - E_3$, where E_n is the energy of the film with n atomic layers of Pr_2O_3.

High concentration of Si in the silicate is stabilized if the Si atoms are intercalated between Pr_2O_3 planes. An example of such a structure, with Si/Pr ratio of 3, is shown in Fig. 4d. The structure is stable above $\mu \simeq 0.5$. Note that not all SiSi bonds in the silicate are oxidized. Oxidation of all these bonds may be difficult without simultaneous excessive oxidation of the substrate: the energy gain is comparable for both processes and the concentration of SiSi bonds is much higher in the silicon than in the silicate.

The presence of such a partially ordered silicate explains the recovery of the substrate-determined orientation in the Pr_2O_3 film grown on top of the apparently amorphous interfacial layer. This recovery is clearly visible in TEM images and in XRD rocking curves.

How does SiO_2 enter the growing film? We found that SiO_2 moieties are stable on the surface of a single Pr_2O_3 monolayer if the oxygen potential is in the range of the oxygen energies in the surface Si–Si bonds. They can be overgrown with Pr_2O_3, leading to silicate formation from the very begining. Comparison of energies and geometries of other structures computed by us indicates that the overgrowth process may be complicated: when the growth of a Pr_2O_3 plane is not yet complete and the surface is rough, or when the amount of SiO_2 is not high enough to build an intercalating plane without inducing a strong deformation to the capping Pr_2O_3 plane, then SiO_2 moieties tend to segregate to the surface. After the topmost Pr_2O_3 plane is closed or enough SiO_2 is collected, the silica units move under the surface in order to maximize the number of Pr–O–Si bonds.

6 Defects and Charge Traps

Reloadable charge can be trapped by electrically neutral defects which have electron transition levels in the forbidden energy range. A Si dangling bond, if not associated with Pr, acts as this kind of trap. Also oxygen vacancy in Pr_2O_3 introduces a reloadable trap state. Life time of charge localized on such trap sites at the interface or in an ultrathin film is limited because the carrier can tunnel away to the substrate. Fixed charge can exist even in an ultrathin film when the relevant transition levels are degenerate with Si bands. Examples of such fixed charge traps in Pr_2O_3 are Pr vacancy, Pr interstitial, and O interstitial.

We calculated the formation energies and electronic structures of fundamental point defects in Pr_2O_3. The Frenkel pair formation energy is about 5 eV in the metal sublattice and 6 eV in the oxygen sublattice. Pr vacancy introduces states close to the valence band (VB) top and may exist in -3 charge state. Pr interstitial introduces states close to the conduction band (CB) bottom and may exist in +3 charge state. O interstitial introduces states close to the VB top and may exist in -2 charge state. Finally, O vacancy introduces midgap states and may exist in +2 charge state.

We will now roughly estimate the lower limit of the interfacial density of misfit Si dangling bonds. We approximate the film/interface/substrate system by a sum of three components: (1) completely relaxed film with rigid lattice, (2) partially relaxed interfacial layer of a given thickness, with lattice constant matching a certain multiplicity of the substrate lattice constant, and (3) rigid substrate. The strained layer is assumed to be compressed, so that one expects formation of dangling bonds in the substrate (the substrate has more surface orbitals than needed for bonding with the layer). Moreover, we assume that all atomic planes in the layer relax in identical way. We also ignore misfit defects between the strained layer and the relaxed film, because the need to create such defects only increases the effective stiffness of the layer, facilitating the formation of Si dangling bonds. Elastic energy of this system can be written in terms of elastic constants of the film (energy stored in the layer), force constant for deviations from the ideal alignment of “connecting points” between the layer and the substrate (interface “friction” energy), and the matching period of the substrate and the strained layer. The energy change upon relaxation enabled by an array of mismatch defects should be compared to the formation energy of such a defect.

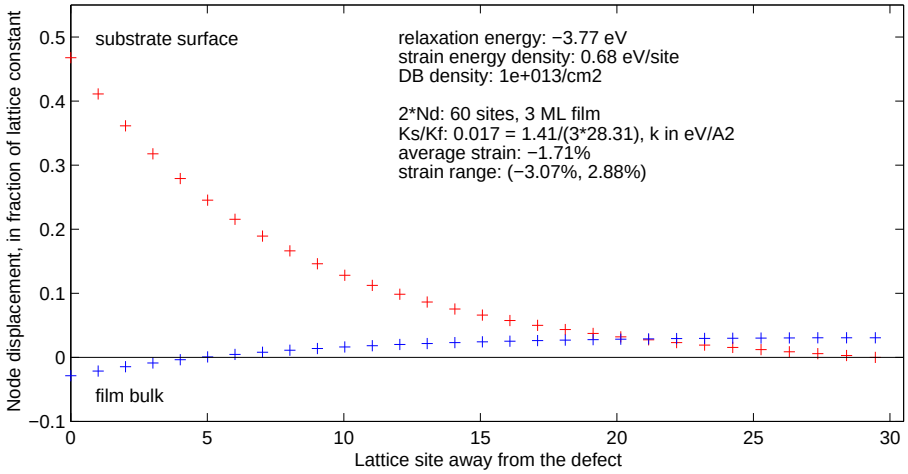

Figure 5. Interface friction model of dangling bond creation at Pr_2O_3/Si(001) interface. Crosses indicate the strain at each connection node. Blue crosses refer to strain in the film, red crosses indicate the strain in the interfacial plane. The interface friction constant has been obtained for the chemically sharp interface 0(SiPr), Fig. 1b. Note that the strain field induced by the defect (node 0) extends only to 20–30 nodes.

The computed friction force constant is small (k_s=1.4 eV/Å), an order of magnitude smaller than typical bond stretching constants in covalent crystals. Assuming that the interfacial Pr_2O_3 is described by the bulk elastic constants, that the lateral relaxation proceeds along one direction, and approximating the plane-strain force constant of the film by

$$k_f = \frac{BA_{latt}}{3(1-\nu)(1-2\nu)} = 28.31\,\mathrm{eV/\AA}^2, \qquad (3)$$

where B = 280 Gpa and A_{latt} = 11.07 Å are computed values and ν is the Poisson ratio assumed to be 1/3, we conclude that while a 2 monolayer (ML) thick film cannot relax through interfacial defect formation, a 3 ML film stores enough energy to create one misfit defect (with formation energy of 1–2 eV) per about 15 lattice sites ($2{\cdot}10^{13}\,\mathrm{cm}^{-2}$. Fig. 5 illustrates that relaxation around an interface dangling bond extends to about 20–30 lattice sites; this is the reason why a 2 ML film cannot relax through interfacial defects.

This result means that a Pr_2O_3 film grown directly on Si(001) would induce an unacceptably high density of interfacial defects. Therefore, an interfacial silicate layer seems to be necessary. The stress may be relieved in the intercalate planes without formation of interfacial dangling bonds. However, the Si content in the silicate should be kept low enough (Pr/Si ratio $\sim$ 1) to eliminate the hazard of formation of Si–Si bridges in the film.

7 Summary and Conclusions

We performed *ab initio* total energy calculations for Pr_2O_3 bulk and Pr_2O_3/Si(001) interfaces, obtaining a number of data helpful in the understaining of the processes responsible for the electrical quality of the films produced for CMOS applications, and providing some guidance for further experimental work.

We obtained fundamental information on native point defects in bulk Pr_2O_3. We found that Pr vacancies and O interstitials would introduce fixed negative charge in the film, Pr interstitials would introduce fixed positive charge, while O vacancies would be amphoteric.

We established a fundamental atomic model for the interface and we examined the energetics of the interface oxidation and reduction. We found that SiO_2 moieties are thermodynamically unstable in SiO_x under Pr_2O_3(110)/Si(001) and dissolve in the Pr oxide. It is plausible that the structure of the resulting silicide is quasi-crystalline and intercalated, with Si/Pr ratio as high as 3. Calculation of interfacial friction between Pr_2O_3 and Si(001) allowed us to estimate the lower bound for interfacial misfit dangling bonds when the film contains no SiO_2 admixture. We conclude that such films would have an unacceptably high density of interfacial dangling bonds. A silicate layer is expected to improve the situation, but the Si content in the silicate should be kept around 1 to avoid the hazard of Si–Si bridge formation in the film, since such bridges can be broken and trap charge.

References

1. G. D. Wilk, R. M. Wallace, and J. M. Anthony, J. Appl. Phys. **89**, 5243 (2001).
2. H. J. Osten, J. P. Liu, P. Gaworzewski, E. Bugiel, and P. Zaumseil, IEDM-2000 Technical Digest, p. 653 (2000).
3. H.-J. Müssig, H. J. Osten, E. Bugiel, J. Dąbrowski, A. Fissel, T. Guminskaya, K. Ignatovich, J. P. Liu, B. P. Zaumseil, and V. Zavodinsky, Proceedings of the 2001 IEEE Integrated Reliability Workshop, p.1 (2001).
4. S. Jeon and H. Hwang, Appl. Phys. Lett. **81**, 4856 (2002).
5. A. Fissel, J. Dąbrowski, and H.-J. Osten, J. Appl. Phys. **91**, 8986 (2002).
6. D. Schmeißer, Matterials Science in Semiconductor Processing **6**, 59 (2003).
7. H.-J. Müssig, J. Dąbrowski, K. Ignatovich, J. P. Liu, V. Zavodinsky, and H. J. Osten, Surf. Sci. **504C** 159 (2002).
8. H.-J. Müssig, J. Dąbrowski, K. Ignatovich, J. P. Liu, V. Zavodinsky, and H.-J. Osten, Solid State Phenomena **82-84** 783 (2002).
9. D. Schmeißer, J. Dąbrowski, and H.-J. Müssig, MRS Proc. Vol. **765**, D3.24 (2003).
10. D. Schmeißer, H.-J. Müssig, and J. Dąbrowski, E-MRS Spring Meeting, Symposium I, June 2003, to appear in Materials Science and Engineering B, (2003).
11. M. Bockstedte, A. Kley, J. Neugebauer, and M. Scheffler, Comp. Phys. Comm. **107**, (1997) 187.
12. D.M Ceperley and B.J. Alder, Phys. Rev. Lett. **45** (1980) 567.
13. J. P. Perdew and A. Zunger, Phys. Rev. B **23**, 5048 (1981).
14. D. R. Haman, Phys. Rev. B **40**, 2980 (1989).
15. G. B. Bachelet, D. R. Hamann, and M. Am Schlüter, Phys. Rev. B **26**, 4199 (1982).
16. J. Dąbrowski, V. Zavodinsky, and A. Fleszar, Microel. Reliability **41**, 1093 (2001).
17. V. G. Zavodinsky and J. Dąbrowski, in preparation.
18. H. Bergman, "Gmelin Handbuch der Anorganischen Chemie, Seltenerdelemente, Teil C1" (Springer-Verlag, Berlin 1974).
19. M. Gasgnier, G. Schiffmacher, P. Caro, and L. Eyring, J. of the Less-Common Metals **116**, 31 (1986).
20. M. Yu. Sinev, G. W. Graham, L. P. Haack, M. Shelef, J. Mater. Res. **11**, 1960 (1996).
21. Y. Wilbert, A. Duquesnov, F. Marion, Compt. Rend. C **264**, 316 (1967).